Results in Materials 15 (2022) 100320

Contents lists available at ScienceDirect

Results in Materials

journal homepage: www.sciencedirect.com/journal/results-in-materials

Defect behaviour in the MoNbTaVW high entropy alloy (HEA)

A.X. Lin-Vines [a], J.A. Wilson [a], A. Fraile [a], Lee J. Evitts [a], M.J.D. Rushton [a], J.O. Astbury [b], W.E. Lee [a], S.C. Middleburgh [a,*]

[a] Nuclear Futures Institute, Bangor University, Dean Street, Bangor, LL57 2DG, United Kingdom
[b] Tokamak Energy Ltd, 173 Brook Drive, Milton Park, Oxfordshire, OX14 4SD, United Kingdom

ARTICLE INFO

Keywords:
High entropy alloy
Defect behaviour
Atomistic modelling
Radiation damage
Defect formation

ABSTRACT

The intrinsic defect formation in the MoNbTaVW HEA is investigated using atomic scale modelling, the goal being to assess its response to radiation damage in its possible use as plasma facing material for fusion reactors. When interstitial defects were modelled, a strong preference to form split interstitial defects containing vanadium was observed, even forming when other interstitial elements were initially placed into the structure. Vacancies and Frenkel pair formation are also modelled and discussed. The distinct behaviour of defects in this HEA has implications for this system as well as related HEAs and their use in nuclear components.

First wall plasma facing materials for fusion reactors are subjected to some of the most extreme temperatures and conditions of any engineered component. Ideal candidates must possess high melting temperatures [1], high thermal conductivity [2], low sputtering erosion rates [3], and ideally small tritium retention [3]. The leading contender material for plasma facing components is tungsten (W) which provides the necessary properties but only for limited exposures. Its poor fracture toughness, high brittle-to-ductile transition temperature (DBTT) [4] and the potential to form an active dust [5], imposes limitations to its operating window in proposed fusion reactor designs. As such, alternatives are being sought.

HEAs are being considered for nuclear applications due to their combination of desirable properties [6] which can include high strength-to-weight ratio [7], fracture toughness and tensile strength [8], corrosion resistance [9], potential low thermal neutron capture cross section [10], and radiation resistance [11]. Importantly, their properties can be tailored due to their considerable compositional flexibility [12]. HEAs also have potential benefits related to radiation damage tolerance and the retention of adequate mechanical properties [11] garnering particular interest of their role for nuclear applications.

One of the main consequences of high energy radiation is the formation of defects within a crystalline lattice. The damage can be categorised by two regimes: the initial defects created as a result of the radiation event (e.g. a cascade) and, after recombination and annihilation of many defects, the residual defect population that remains. It is this residual defect population that impacts the long-term behaviour of the material as they alter properties mediated by phonons (e.g. thermal properties), mechanical properties and transport mechanisms. In this study, we investigate the intrinsic defect formation in the equiatomic BCC MoNbTaVW model alloy to begin to assess the radiation damage response of this and similar HEAs. In particular, we highlight a novel mechanism in interstitial defects that may alter the radiation tolerance of HEAs.

The particular HEA composition is chosen for:

- the presence of tungsten which provides the benefits of high strength at high temperatures [11].
- the use of vanadium, which Yin et al. determined to improve the strength of this due to its large misfit volume in crystalline structures [13].
- Xia A et al. demonstrated the thermal stability of this composition up to 1500 °C which is ~400 °C higher than pure tungsten's recrystallisation temperature [14].

This investigation employed density functional theory (DFT), using the Vienna Ab initio Simulation Package (VASP) [15,16]. Simulations were performed under constant pressure, allowing the cell volume and shape to relax as well as the atomic positions. Methfessel-Paxton smearing with a smearing width of 0.1 eV. Cut-off energy of plane waves were 500 eV and a 4×4×4 *k*-point mesh was used providing an accuracy better than 0.01 eV in the system's total energy. The cut-off energy for electronic minimization was set to 10^{-4}eV and geometry

* Corresponding author.
E-mail address: s.middleburgh@bangor.ac.uk (S.C. Middleburgh).

https://doi.org/10.1016/j.rinma.2022.100320
Received 13 June 2022; Received in revised form 12 August 2022; Accepted 29 August 2022
Available online 2 September 2022

optimization cut-off value for minimization was set to 10^{-3} eV/Å generalised gradient approximation (GGA) exchange correlation was used as determined by Perdew Burke and Ernzerhof [17]. The pseudo-potential library provided with VASP 5.4.4 was used.

Special quasi-random structures (SQS) [18] were used to produce ten 3×3×3 BCC supercells of MoNbTaVW containing 54 sites to which the alloy's elements were assigned (Fig. 1 shows an example structure).1.5 times the lattice constant was used to determine pair correlation functions, so up to and including the 3rd nearest neighbour. Triplet correlation functions were not considered. Larger systems should be considered in future work to assess the impact of elastic finite size effects [19], as assessed previously by Burr et al., however, due to computational constraints and the number of calculations required to attain suitable statistics for this work, the 3×3×3 was deemed sufficient. The smallest supercell that allows true equiatomic concentrations to be considered is the 5×5×5 supercell containing 250 atoms, a size of supercell not reasonable for the number of calculations required in this investigation. Past work has assessed non-equiatomic systems and shown the impact in these alloy systems is small [20]. In the perfect system, 11 of each element was included in the system apart from Ta that had 10 atoms present (totalling the 54 lattice sites in the system).

SQS cells with the perfect structure were simulated, and the lattice positions of the elements and lattice parameter of the cell was allowed to relax. The average lattice parameter at 0 K was computed to be 3.19 ± 0.01 Å. Byggmaster et al. calculated the MoNbTaVW lattice parameter at 3.195 ± 0.001 Å [21] with an empirical potential. Experiments performed by Senkov et al. reported a value 3.187 Å [22].

The enthalpy of formation of the HEA with respect to the individual metallic components was computed to be −0.04 eV per atom (averaging over the 10 SQS structures produced) highlighting the stability of the alloy [12]. Larger supercells containing 128 atoms were briefly considered and formation energies were within 0.01 eV (averaged over 10 systems) of those computed with the smaller cell, highlighting the suitability of the smaller supercell.

Vacancy calculations were performed by removing a single atom to create a new 53-atom supercell. This method was repeated to produce 54 unique supercells. Similarly, isolated interstitials were considered in the HEA structure. Each perfect 54-atom supercell has a single atom added into predefined locations as interstitials to form a 55-atom supercell. Ten different cells were generated per element considered totalling 50 interstitial simulations.

The vacancy formation energy (E_{Vac}) is given by Ref. [23]:

$$E_{Vac} = E_{Defective} + E_{Metal} - E_{Perfect} \quad \text{Eq (1)}$$

where a system containing a vacancy ($E_{Defective}$) was created forming its individual metal (E_{Metal}) from a perfect supercell ($E_{Perfect}$). The relaxed structures showed simple vacancy defects formed in each case (no evidence of split vacancies or extensive restructuring). Table 1 reports the vacancy formation energies computed for each species forming a unit of its metal (in each case energies were generated for the perfect BCC metal). For comparison, the table provides the vacancy formation energies of each type in the pure metals from literature. The standard error was calculated by taking the mean of the errors associated with each vacancy formation energy for each element.

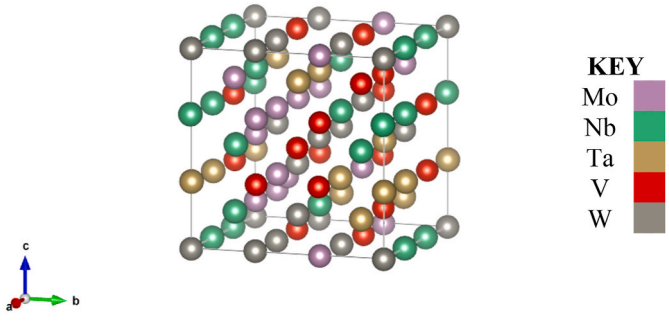

Fig. 1. Special quasi-random structure (SQS) supercell of near equiatomic MoNbTaVW.

Table 1
Vacancy formation energy of pure elements with previous FP-LMTO experimental and DFT experimental values. Supercells size for simulated DFT of N = 54 and FP-LMTO N = 27 with BCC metals.

Element	Average Vacancy Formation Energy (eV)	Vacancy in monoatomic metal (eV)
Mo	3.67 ± 0.25	2.61 [24], 3.13 [25]
Nb	3.33 ± 0.23	2.31 [26], 2.92 [25]
Ta	3.54 ± 0.34	3.49 [25]
V	3.43 ± 0.15	3.06 [25]
W	3.48 ± 0.29	2.95 [27], 3.27 [25]

[24] Einstein crystal method
[25] DFT calculations using the LDA exchange correlation.
[26] DFT calculations using VASP with the GGA of Perdew and Wang (PW91).
[27] DFT calculations using VASP with the GGA-PBE exchange correlation.

The vacancy formation energy of the system can be assessed with respect to forming a unit of HEA instead of the individual metal, more akin to a Schottky formation energy (i.e. a unit of material is removed instead of a single atom leaving a stoichiometric defective system). A value of 3.48 ± 0.27 eV was computed which compares very closely to the scaled average of the values in Table 1 (3.49 eV), which is to be expected given the low reaction energy between the constituent species reported earlier (−0.04 eV per atom).

The predicted vacancy formation energies in this HEA are higher than those reported in the individual metal systems when compared to previously published work including that of Korhonen et al. [25], indicating a deviation in the expected behaviour, potentially resulting from a change in bonding in the system, possibly associated with intermetallic compounds. The Schottky and vacancy formation energy calculated in this high entropy alloy is larger than the vacancy formation energy calculated for W using similar methods [27] and as such one may expect some improvements in high temperature behaviour and lower intrinsic defect populations [28].

Significant relaxation and restructuring of interstitial defects was observed when inserting elements in as a simple tetrahedral or octahedral interstitial. 74% of the resulting relaxed structures are split-interstitials, where two interstitial species share a single lattice site. More intriguingly, 70.3% of the split interstitials were vanadium-vanadium split interstitials. Further inspection of the relaxed interstitial structures shows a distinct behaviour: 91.8% of the relaxed interstitials involved a vanadium, either as part of a split-interstitial or crowdion [31] cluster, or as an isolated vanadium interstitial.

Fig. 2 illustrates a typical simulation that highlights how a Ta atom added to an octahedral site displaces an adjacent vanadium atom out of its lattice site to form a split interstitial. As can be seen, the atom identified as Ta moves onto a site previously occupied by a vanadium which forms a split-interstitial with another vanadium.

This barrierless restructuring of interstitial defects highlights a key, distinct behaviour difference between these HEAs and single metal systems (and systems with a dominant element) that will impact the defect population by increasing the barrierless recombination volume of defects, thus reducing residual defects. Other mechanisms in HEAs may compete with this process, such as local trapping of defects in deep energy wells, but if ubiquitous in HEAs, the mechanism may be able to be enhanced or amplified to further improve radiation damage by careful selection of constituent species.

By considering the vacancy and interstitial defects together, the Frenkel formation energy can be computed. Accommodation mechanisms for the additional atoms were compared in Fig. 3. The Frenkel formation energy averaged for each defect that formed, and the frequency of each defect as a percentage of those observed is reported. As

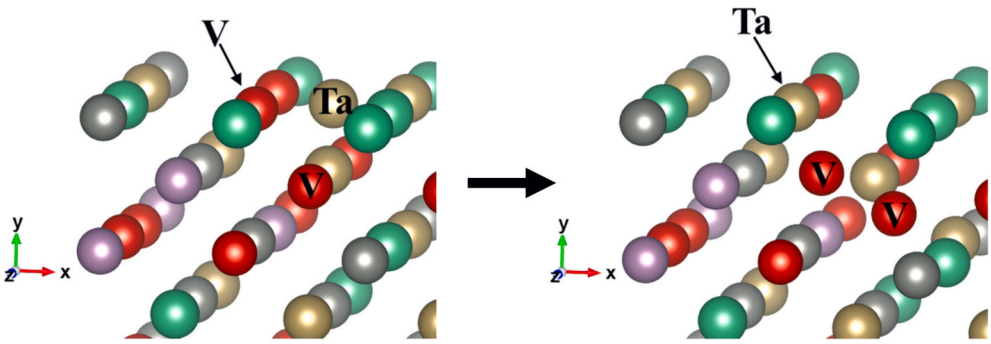

Fig. 2. Relaxation forming a split interstitial made of two vanadium atoms after a tantalum atom was placed as an interstitial defect.

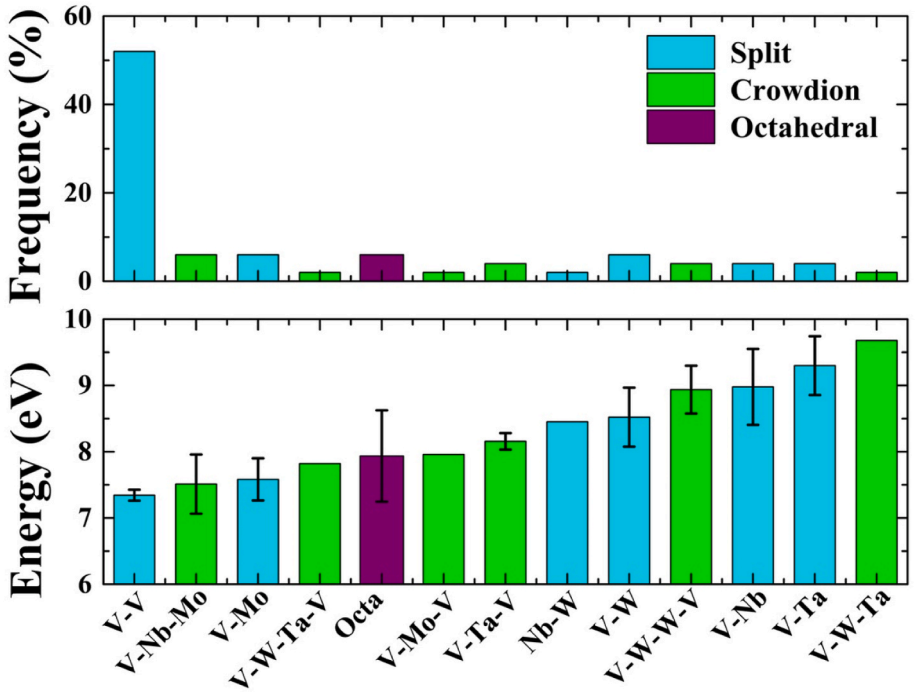

Fig. 3. – (Top) Frequency of defects observed after system optimization with an interstitial species. (Bottom) Average defect formation energy of every observed interstitial defect after relaxation. The standard error has been calculated for each defect type observed. Defects only observed once have no error bar associated with them.

can be expected, the V–V split interstitial that was observed to form more frequently is also predicted to be most favourable with an average of 7.34 ± 0.42 eV.

In a similar manner to the computation of the vacancy formation energies, the anti-Schottky or interstitial formation energy can be computed (taking a unit of HEA and accommodating it interstititally). The anti-Schottky energy is computed to be 3.79 ± 0.23 eV, similar to that but larger than the computed Schottky energy (3.48 ± 0.27 eV).

To conclude, the intrinsic defect behaviour in the MoNbTaVW HEA has been assessed and distinct differences are observed when compared to simple metals such as tungsten. The key findings are as follows:

- The most favoured intrinsic defect is predicted to be the vacancy/Schottky defect with a formation energy of 3.48 ± 0.27 eV per atom. The predicted concentration of vacancies under equilibrium conditions could be expected to be lower than that of W, which has a lower vacancy formation energy [27]. The distribution in energies within the HEA compared to a single element system is not expected to impact the overall defect population considerably. The anti-Schottky energy (forming interstitials) has a similar energy: 3.79 ± 0.23 eV.
- Frenkel pair formation is predicted to proceed with formation energies >7 eV.
- When interstitial defects were considered, a clear preference for the formation of split interstitial defects was observed, consistent with other atomic scale studies of BCC systems [29].
- Vanadium was the most common and most favourable interstitial defect species after relaxation, forming split interstitial defects, regularly forming when other interstitial defects were originally placed into the structure. Vanadium is the metal with the smallest atomic radius in the composition considered, which may explain the observations (causing less steric disturbance). It will be of value for future work to understand whether the ease of formation of interstitials in HEAs can be linked to something as simple as metallic radius. Vanadium is described as a great strengthening addition to HEAs by Yin et al. [13]. The preferential formation of vanadium split interstitials over any of the other species may provide a mechanism for the observed strengthening in the material. Further work building from this result will be carried out assessing the defect's impact on mechanical properties of the material and the alteration to dislocation behaviour.

- Interstitials have been observed to displace and migrate with no energy barrier beyond their nearest neighbour position. This highlights that the recombination volume of interstitials is expected to be larger compared to a single element system (or alloy dominated by one element). As such, Frenkel pairs and radiation damage caused by a cascade or thermal spike within the material are expected to annihilate more frequently, leaving a lower residual defect population within the HEA, improving the material's response to radiation. Further work is required to assess the role of initial interstitial species on the final defect species population – a task that will require larger numbers of calculations, potentially aided by the use of more computationally efficient empirical potentials.

Declaration of competing interest

The authors declare the following financial interests/personal relationships which may be considered as potential competing interests:

Alexander Lin-Vines reports financial support was provided by Tokamak Energy Ltd. Simon Middleburgh reports financial support was provided by Tokamak Energy Ltd.

Acknowledgments

SCM, WEL and MJDR are part of the Sêr Cymru II project (80761-BU-103), funded by the Welsh European Funding Office (WEFO) part of the European Regional Development Fund (ERDF). We would like to acknowledge the support of the Supercomputing Wales (SCW) project, which is part-funded by the ERDF via the Welsh Government. We would also like to acknowledge the support of the Knowledge Economy Skills Scholarships (KESS 2) which is a pan-Wales higher level skills initiative led by Bangor University on behalf of the HE sector in Wales. It is part funded by the Welsh Government's European Social Fund (ESF) convergence programme for West Wales and the Valleys. We would also like to acknowledge David Kingham, from Tokamak Energy, whose support has been hugely beneficial to the Nuclear Futures Institute, based at Bangor University, and this work.

References

[1] R. Johnson, Point-defect calculations for tungsten, Phys. Rev. B 27 (1983), 2014.
[2] P. Zacha, S. Entler, High heat flux limits of the fusion reactor water-cooled first wall, Nucl. Eng. Technol. 51 (5) (2019) 1251–1260.
[3] J. Bookes, J. Allain, R. Doerner, A. Hassanein, R. Nygren, T. Rognlien, D. Whyte, Plasma–surface interaction issues of an all-metal ITER, Nucl. Fusion 49 (2009), 035007.
[4] A. Wronski, A. Foudeux, The ductile-brittle transition in polycrystalline tungsten, J. Less Common Met. 8 (3) (1965) 149–158.
[5] E. Fortuna-Zaleśna, et al., Studies of dust from JET with the ITER-Like Wall: composition and internal structure, Nuclear Materials and Energy 12 (2017) 582–587.
[6] E. Pickering, A. Carruthers, P. Barron, S. Middleburgh, D. Armstron, A. Gandy, High-entropy alloys for advanced nuclear applications, Entropy 21 (2021) 98.
[7] K. Youssef, A. Zaddach, C. Niu, D. Irving, C. Koch, A novel low-density, high-hardness, high-entropy alloy with close-packed single-phase nanocrystalline structures, Materials Research Letters 3 (2) (2014) 95–99.
[8] M. Siefi, D. Li, Z. Yong, P. Liaw, J. Lewandowski, Fracture toughness and fatigue crack growth behavior of as-cast high-entropy alloys, J. Occup. Med. 67 (2015) 2288–2295.
[9] Y. Qiu, M. Gibson, H. Fraser, N. Birbilis, Corrosion characteristics of high entropy alloys, Mater. Sci. Technol. 31 (2015) 1235–1243.
[10] D. King, S. Cheung, S. Humphry-Baker, C. Parkin, A. Couet, M. Cortie, G. Lumpkin, S. Middleburgh, A. Knowles, High temperature, low neutron cross-section high-entropy alloys in the Nb-Ti-V-Zr system, Acta Mater. 166 (2019) 435–446.
[11] O. El-Atwani, et al., Outstanding radiation resistance of tungsten-based high-entropy alloys, Sci. Adv. 5 (2019) 1–9.
[12] D. King, S. Middleburgh, A. McGregor, M. Cortie, Predicting the formation and stability of single phase high-entropy alloys, Acta Mater. 104 (2016) 172–179.
[13] B. Yin, F. Maresca, W. Curtin, Vanadium is an optimal element for strengthening in both fcc and bcc high-entropy alloys, Acta Mater. 188 (2020) 486–491.
[14] A. Xia, R. Franz, Thermal stability of MoNbTaVW high entropy alloy thin films, Coatings 10 (2020) 941.
[15] G. Kresse, J. Furthmüller, Efficiency of ab-initio total energy calculations for metals and semiconductors using a plane-wave basis set, Comput. Mater. Sci. 6 (1) (1996) 15–50.
[16] G. Kresse, J. Hafner, Ab initio molecular dynamics for liquid metals, Phys. Rev. B 47 (1993), 558(R).
[17] J. Perdew, K. Burke, M. Ernzerhof, Generalized gradient approximation made simple, Phys. Rev. Lett. 77 (1996) 3865.
[18] A. Zunger, S.-H. Wei, L. Ferreira, J. Bernard, Special quasirandom structures, Phys. Rev. Lett. 65 (1990) 353.
[19] P. Burr, M. Cooper, Importance of elastic finite-size effects: neutral defects in ionic compounds, Phys. Rev. B 96 (2017), 094107.
[20] S. Middleburgh, D. King, G. Lumpkin, Atomic scale modelling of hexagonal structured metallic fission product alloys, R. Soc. Open Sci. 2 (4) (2015), 140292.
[21] J. Byggmästar, K. Nordlund, F. Djurabekova, Modeling refractory high-entropy alloys with efficient machine-learned interatomic potentials: defects and segregation, Phys. Rev. B 104 (2021), 104101.
[22] O. Senkov, G. Wilks, J. Scott, D. Miracle, Mechanical properties of Nb25Mo25Ta25W25 and V20Nb20Mo20Ta20W20 refractory high entropy alloys, Intermetallics 19 (5) (2011) 698–706.
[23] Y. Pan, Y. Lin, Influence of vacancy on the mechanical and thermodynamic properties of IrAl3 compound: a first-principles calculations, J. Alloys Compd. 684 (2016) 171–176.
[24] G. Smirnov, V. Stegailov, Formation free energies of point defects and thermal expansion of bcc U and Mo, J. Phys. Condens. Matter 31 (2019), 235704.
[25] T. Korhonen, M. Puska, R. Nieminen, Vacancy-formation energies for fcc and bcc transition metals, Phys. Rev. B 51 (1995) 9526.
[26] A.-Y. Gao, Y.-L. Liu, Z.-H. Dai, C. Duan, Elucidating hydrogen assisting vacancy formation in metals: Mo and Nb as examples, Eur. Phys. J. B 86 (2013) 355.
[27] S. Middleburgh, R. Voskoboinikov, M. Guenette, D. Riley, Hydrogen induced vacancy formation in tungsten, J. Nucl. Mater. 448 (2014) 270–275.
[28] M. Fullarton, R. Voskoboinikov, S. Middleburgh, Hydrogen accommodation in a-iron and nickel, J. Alloys Compd. 587 (2014) 794–799.
[29] D. Nguyen-Manh, A. Horsfield, S. Dudarev, Self-interstitial atom defects in bcc transition metals: group-specific trends, Phys. Rev. B 73 (R) (2006), 020101.